Article

Second-Generation of Tunable pH-Sensitive Phosphoramidate-Based Linkers for Controlled Release

Cindy Jan Choy, Corinne Rose Ley, Austen Lambert Davis, Brian Scott Backer, Jonathan James Geruntho, Brian H Clowers, and Clifford E. Berkman

Bioconjugate Chem., **Just Accepted Manuscript** • DOI: 10.1021/acs.bioconjchem.6b00422 • Publication Date (Web): 26 Aug 2016

Second-Generation of Tunable pH-Sensitive Phosphoramidate-Based Linkers for Controlled Release

Cindy J. Choy†, Corinne R. Ley†, Austen L. Davis, Brian S. Backer, Jonathan J. Geruntho, Brian H. Clowers, and Clifford E. Berkman*

Washington State University, Department of Chemistry, PO Box 644630
Pullman, WA 99164-4630

†Co-first authors

Corresponding author: Clifford E. Berkman, Ph.D.
Corresponding author address: Washington State University
Department of Chemistry
Pullman, WA 99164-4630
Tel: 509-335-7613
Fax: 509-335-8389
Email: cberkman@wsu.edu

Abstract

We have developed a second-generation of tunable pH-sensitive linkers based on our phosphoramidate scaffold to release amine-containing drugs under acidic conditions. The pH-triggered phosphoramidate-based linkers are responsive to pH and do not require intracellular enzymatic action to initiate drug release. Based on the model scaffolds examined, phosphoramidate-based linkers could be selected for particular properties for controlled-release applications such as amine type, stability under physiological conditions, or release rates at various pH values such as intracellular endosomal conditions. Key to the pH-triggered amine release from these linker is a proximal carboxylic acid to promote the hydrolysis of the phosphoramidate P-N bond, presumably through an intramolecular general-acid type mechanism. Phosphoramidate hydrolysis is largely governed by the pKa of the leaving amine. However, the proximity of the neighboring carboxylic acid attenuates the stability of the P-N bond to hydrolysis, thus allowing for control over the release of an amine from the phosphoramidate center. In addition, we observed that the Thorpe-Ingold effect and rigidification of the scaffold could further enhance the rate of release. Esterification of the neighboring carboxylic acid was found to protect the scaffold from rapid release at low pH. This latter observation is particularly noteworthy as it suggests that the phosphoramidate-based drug-conjugate scaffold can be protected as an ester prodrug for oral administration. While the tunability phosphoramidate linkers is attractive for applications in intracellular trafficking studies in which pH changes can trigger the release of turn-on dyes, antibody drug conjugates (ADC), small-molecule drug conjugates (SMDC) and drug eluting stents (DES), the promise of oral delivery of drug-conjugates is expected to have broad impact in applications or controlled-release.

Introduction

The narrow therapeutic window and lack of tumor selectivity of cytotoxic chemotherapy has prompted the emergence of targeted therapeutics that combine the toxicity of a highly-potent chemotherapeutic drug with the specificity of a chemical or biological targeting molecule.[1,2] At present, the field of targeted drug delivery is dominated by antibody drug conjugates (ADCs). Currently, there are over 250 clinical trials representing over 40 unique ADC agents.[3] A critical aspect to effective targeted drug therapies is the controlled release of a cytotoxic drug from the targeting molecule (e.g., antibody) upon cellular internalization or localization. While much attention within the ADC field has been focused on consistently and reliably coupling the drug to the targeting biomolecule,[1,2,4-8] there has been considerably less effort to develop controlled, site-specific chemical release of the cytotoxic drug. The two most common cleavable linkers in the field of ADC is Seattle Genetics' valine-citrulline linker,[9,10] which relies on enzymatic cleavage by cathepsin B in lysosomes, and ImmunoGen's succinimidyl 4-[*N*-maleimidomethyl]cyclohexane-1-carboxylate (SMCC) linker technology. ImmunoGen's SMCC linker technology is not cleavable and therefore restricts its utility to the few drugs that are active as a SMCC-drug conjugate once the antibody has been digested in the lysosome.[10] These linker technologies developed for ADCs necessitate that they be both internalized and processed in the lysosome to release the cytotoxic drug. Due to these requirements, the utility of these linkers is limited to applications for which the drug conjugate is both internalized by endocytosis and is transported to lysosomes. In addition, such linkers do not allow for release under microenvironments of tumor cells to take advantage of the bystander effect.[11,12] Moreover, these linkers cannot be more broadly applied for general controlled release applications such as drug eluting stents.

Other non-proprietary cleavable linkers exist that are labile to the action of glutathione on a disulfide linkage or hydrolysis under acidic conditions. The disulfide linkers rely on higher intracellular glutathione concentration compared to extracellular glutathione level, however, it has been shown to be unstable in circulation due to the presence of glutathione in blood. The most well known acid-labile linker is the hydrazide linker. Pfizer's ADC, Mylotarg, was developed using the hydrazide linkage but the drug was withdrawn from the market, presumably due to premature release prior to full internalization.[13,14]

In summary, the current cleavable linkers for selective drug release are not broadly applicable for targeted therapeutic and controlled-drug release applications. In general, linker technology relies on one of three basic modes of activation: 1) proteolytic action by lysosomal enzymes, 2) glutathione reduction of a disulfide linkage, or 3) hydrolytic degradation under acidic conditions.[15-17] All three modes are designed around specific applications and offer limited control over the release characteristics; tunability of the cleavage kinetics often is dependent only upon steric bulk incorporated into the linker. Consequently, these linkers have significant limitations, particularly in controlled release applications such as drug-eluting stents.

We recently reported a novel phosphoramidate scaffold that can be employed to selectively release amine-containing drugs and/or self-immolating spacers at varying rates dependent upon pH (**Figure 1**, **1-5**).[18] We envision that cleavable linkers based on this scaffold can be tailored for specific requirements of controlled-release applications, such as amine type, stability under physiological conditions, or release rates at various pH conditions. Representative applications for such tunable pH-programmable cleavable linkers include antibody or small-molecule drug conjugates, drug-eluting stents, prodrug activation, as well as intracellular trafficking studies in which pH changes can trigger the release of turn-on dyes.

In our first report, we demonstrated that phosphoramidate hydrolysis was largely governed by the pKa of the leaving amine (e.g., primary, secondary, aniline).[18] However, the proximity of a neighboring pyridine group further attenuated the stability of the P-N bond to hydrolysis, thus allowing for control over the release of an amine from the phosphoramidate center. The proximal pyridinium group promoted the hydrolysis of the phosphoramidate P-N bond, presumably through an intramolecular general-acid type mechanism. The focus of this study was to examine the expected analogous tunability of the phosphoramide scaffold when the neighboring proton donor was a carboxylic acid (**Figure 1**, **6-11**). Again, we examined amines linked to the

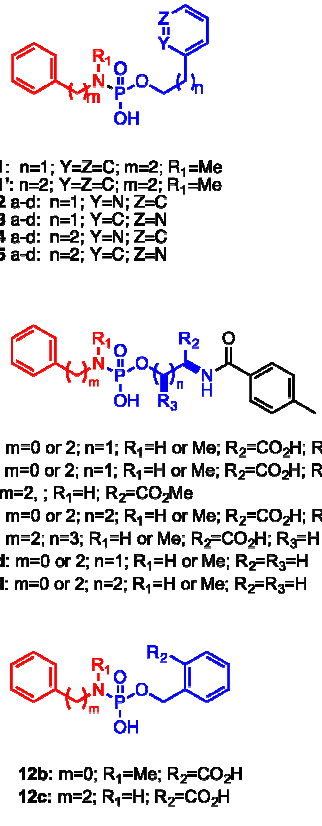

Figure 1. Phosphoramidate-based pH-programmable cleavable linkers.

phosphoramidate core as representative models for drugs or self-immolating spacers that could be released from the phosphoramidate scaffold for relevant controlled-release applications. The specific series of cleavable linker models for this study were phosphoramidates of serine (**6a-d**), threonine (**7a-d** and **7c´**), homoserine (**8a-d**), 5-hydroxynorvaline (**9a-b**), 2-aminoethanol (**10a-d**), 3-aminopropanol (**11a-b**), and 2-(hydroxymethyl)benzoate (**12a,c**) and monitoring the rate of hydrolysis of the P-N bond of model amine-containing drugs at various pH conditions at 37 ^{o}C.

Results and Discussion

A library of representative model drug-linker conjugates based on an acid-sensitive phosphoramidate core (**Figure 1**, **6-12**) was prepared and evaluated for stability at various pH values (3.0 – 7.4). The rationale for the library design was to confirm that phosphoramidates containing a proximal carboxylic acid were susceptible to similar hydrolytic stability as was previously observed for phosphoramidates containing a proximal pyridinium group.[18] Alcohols **14-17** were chosen to test the tunability via the proximity of the carboxylate to the phosphorus center. Alcohols **18-19** were chosen to monitor the stability of phosphoramidates lacking the neighboring carboxylate. Amines **a-d** were selected as representatives of chemotherapeutic drugs typically found in ADCs (e.g., **a** aniline, **c** 1^{o} amine, and **d** 2^{o} amine to mimic a self-immolating spacer, doxorubicin, and MMAE, respectively).

In general, alcohols (**14-19**) were readily prepared from commercially available amino

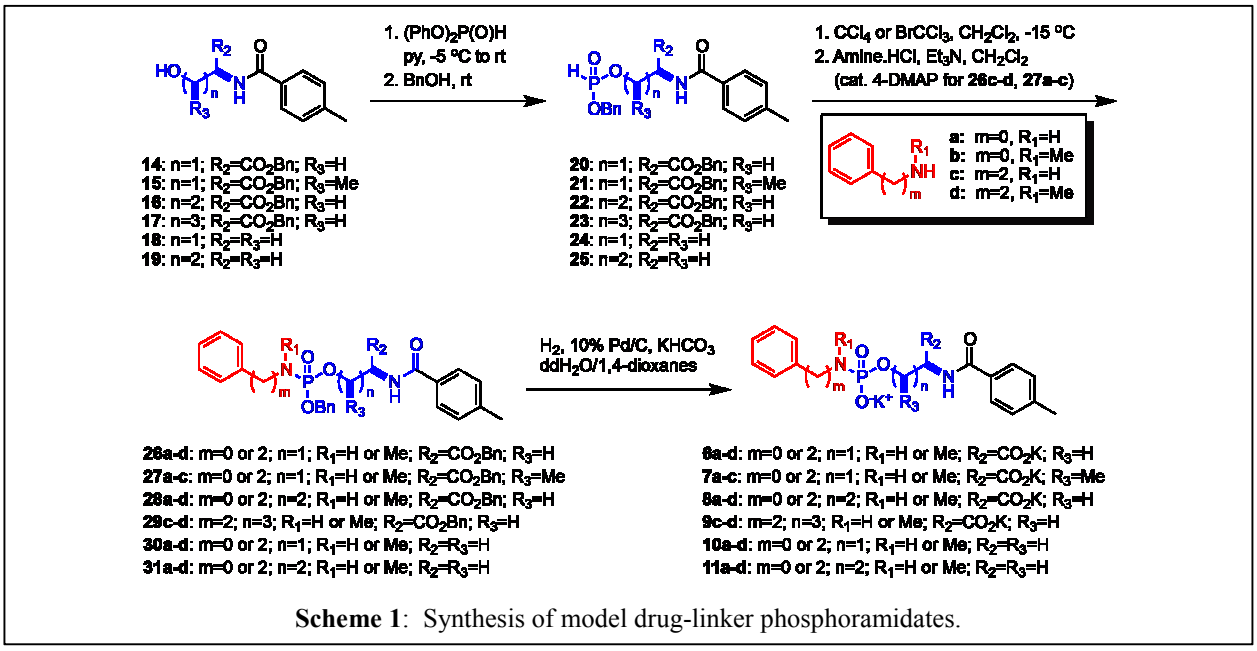

14: n=1; R_2=CO_2Bn; R_3=H
15: n=1; R_2=CO_2Bn; R_3=Me
16: n=2; R_2=CO_2Bn; R_3=H
17: n=3; R_2=CO_2Bn; R_3=H
18: n=1; R_2=R_3=H
19: n=2; R_2=R_3=H

20: n=1; R_2=CO_2Bn; R_3=H
21: n=1; R_2=CO_2Bn; R_3=Me
22: n=2; R_2=CO_2Bn; R_3=H
23: n=3; R_2=CO_2Bn; R_3=H
24: n=1; R_2=R_3=H
25: n=2; R_2=R_3=H

26a-d: m=0 or 2; n=1; R_1=H or Me; R_2=CO_2Bn; R_3=H
27a-c: m=0 or 2; n=1; R_1=H or Me; R_2=CO_2Bn; R_3=Me
28a-d: m=0 or 2; n=2; R_1=H or Me; R_2=CO_2Bn; R_3=H
29c-d: m=2; n=3; R_1=H or Me; R_2=CO_2Bn; R_3=H
30a-d: m=0 or 2; n=1; R_1=H or Me; R_2=R_3=H
31a-d: m=0 or 2; n=2; R_1=H or Me; R_2=R_3=H

6a-d: m=0 or 2; n=1; R_1=H or Me; R_2=CO_2K; R_3=H
7a-c: m=0 or 2; n=1; R_1=H or Me; R_2=CO_2K; R_3=Me
8a-d: m=0 or 2; n=2; R_1=H or Me; R_2=CO_2K; R_3=H
9c-d: m=2; n=3; R_1=H or Me; R_2=CO_2K; R_3=H
10a-d: m=0 or 2; n=1; R_1=H or Me; R_2=R_3=H
11a-d: m=0 or 2; n=2; R_1=H or Me; R_2=R_3=H

Scheme 1: Synthesis of model drug-linker phosphoramidates.

acids and/or amines. To prepare the phosphoramidate models for this study, a common method was employed to install the phosphorus core and enable late-stage diversification with representative amines (**Scheme 1**). Transesterification of diphenyl phosphite by sequential addition of the functionalized alcohol then benzyl alcohol provided H-phosphonates **20-25**, which were then subjected to Atherton-Todd conditions to generate the protected phosphoramidate intermediates **26a-d** through **31a-d**. Global deprotection of these precursors by hydrogenolysis yielded the model drug-linker conjugates **6-11**. Compounds **12 b-c** were synthesized analogously as **6-11** starting with ethyl 2-(hydroxymethyl)benzoate and fluorenylmethanol. Deprotection was achieved with 1M LiOH as previously described.[18]

Once prepared, the stability of the model drug-linker conjugates **6-12** was monitored by ^{31}P NMR at pH 3.0, 5.5, and 7.4 at 37 ^{o}C. The NMR array data was compiled using Mnova 10.0 software (Mestrelab Research, Escondido, CA), and the hydrolytic drug release of the respective amine was analyzed in comparison to a constant concentration of the external standard triphenylphosphine oxide (**Figure 2A**). The peak area for each compound was normalized to the standard over 8 h, and the rate of hydrolysis followed first order kinetics (**Figure 2B**).

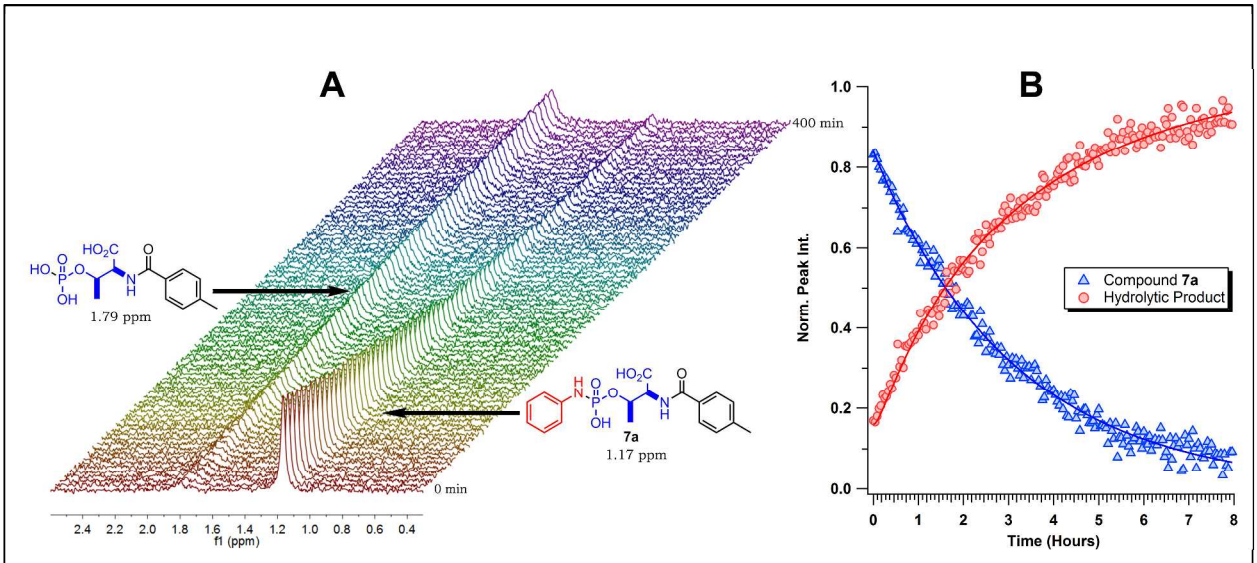

Figure 2. (**A**) Raw stacked NMR data for **7a** (1.17 ppm) at pH 5.5. The peak at 1.79 ppm is the hydrolytic product. (**B**) Compiled and fitted data for the area of **7a** (blue) normalized to the standard and its hydrolytic product (red).

As expected, the hydrolysis rates of our second-generation models (**Figure 3**) were largely influenced by two distinct elements: 1) the type of amine (e.g. primary, secondary, aniline, secondary aniline), and 2) the proximity of the carboxylic acid to the phosphorus center. Previously we reported that the structure of the amine impacts hydrolysis of the P-N bond such that *N*-methylphenethylamine > *N*-methylaniline > phenethylamine > aniline. This trend was again observed for each series of model drug-linker phosphoramidates in this study. For example, when comparing compounds **8a-d**; hydrolysis at pH 5.5 is most rapid for **8d** (6.6 h) while no detectable hydrolysis was observed for **8a** over 8 h. The trend was further illustrated by hydrolysis of control compounds **10a-d**, which lack the carboxylic acid, but displayed notable decomposition at pH 3.0 where **10d** > **10b** > **10c** > **10a**.

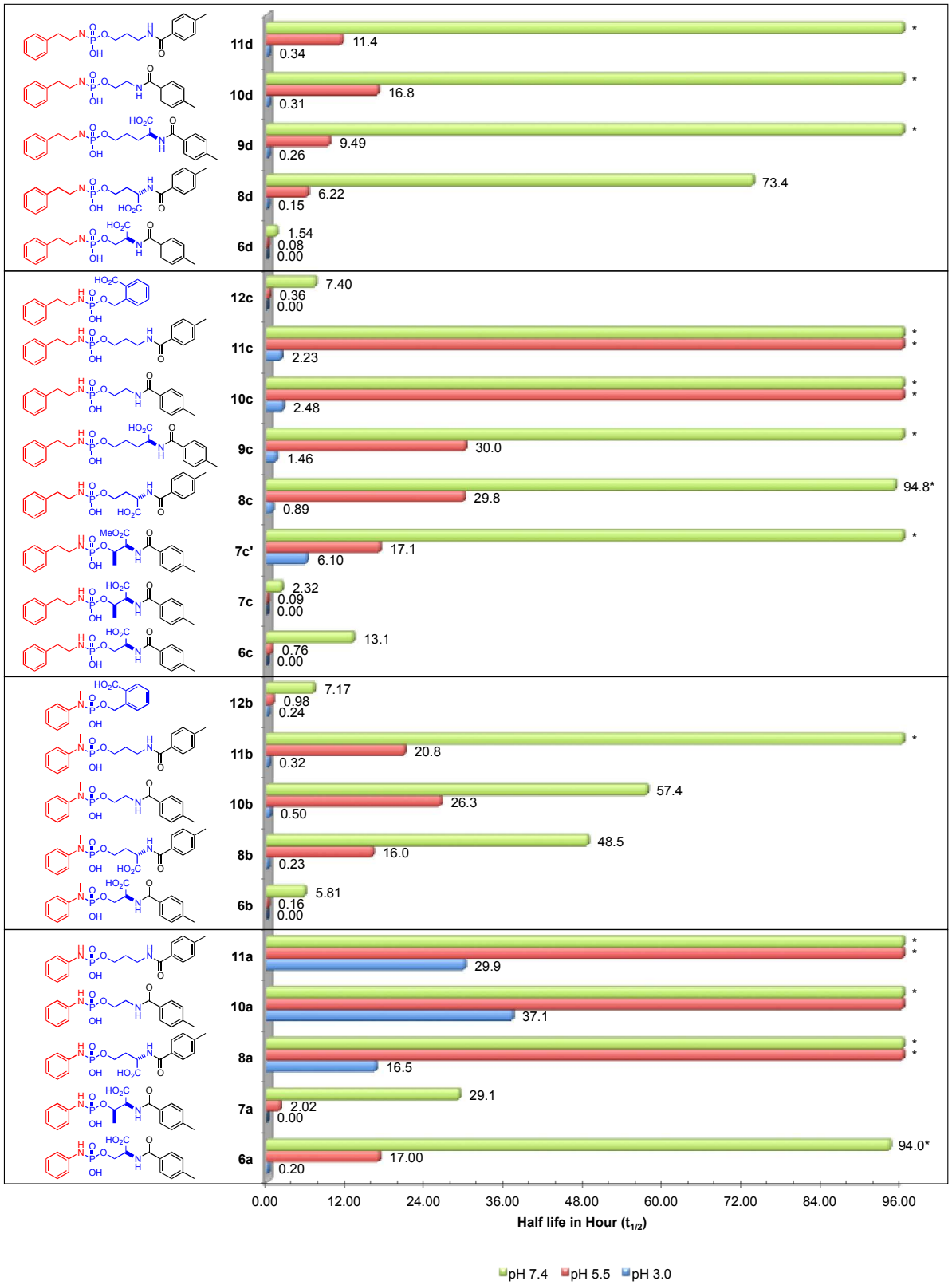

Figure 3: Stability of model drug-linker phosphoramidates at pH 3.0, 5.5, and 7.4 (37 °C). *No detectable hydrolysis observed over 8 hrs.

While phosphoramidates are generally unstable under highly acidic conditions, the presence of a neighboring acidic group is essential for the unusual lability of the P-N bond under mild pH conditions. This is evident by the rapid hydrolysis of **6a-d** and **8a-d** relative to their respective control compounds **10a-d** and **11c-d**, which lack a proximal carboxylic acid. The serine-derived compounds **6c-d** were particularly unstable as the ^{31}P FID could not be acquired at pH 3.0 due to complete hydrolysis of the phosphoramidates in less than 5 min. Similarly, compounds **8c-d** show an approximately 2-fold increase in the rate of hydrolysis relative to the control compounds **11c-d**, which lack a proximal carboxylic acid.

The stability profiles of our model drug-linker conjugates support our hypothesis that the proximity of the neighboring acidic group (e.g., carboxylic acid) to the phosphorus centers strongly influences the rate of hydrolysis of the P–N bond. As the distance is increased in the phosphoramidates based on serine (**6a-d**, n=1), homoserine (**8a-d**, n=2), and 5-hydoxynorvaline (**9c-d**, n=3), the hydrolytic stability also increases at all pH values examined. This was previously observed in both our preliminary studies with carboxylate-containing phosphoramidates as well as our first-generation pyridinium scaffolds.[18] In fact, extending the distance of the carboxylate from 1 to 3 methylene units (e.g., **9c-d**) resulted in a model drug-linker conjugates with similar stability profile as the control compound that lack a neighboring carboxylic acid.

As discussed in our previous report,[18] the data herein appear to be consistant with an intramolecular general-acid mechanism to explain the influence that the neighboring carboxylate exerts on the hydrolysis rate of the phosphoramidate P-N bond. We initially proposed such a mechanism for the pryidinium-based scaffolds,[18] which could also explain the pH-stability trends of our current carboxylate-based scaffolds (**Scheme 2A**). Intramolecular general-acid mechanisms are known to facilitate various chemical transformations[19-23] and we recently proposed this for the hydrolysis of the P-N bond in phosphoramidates possessing a pyridininium group proximal to the central phosphorus atom.[18] It is understood that at physiological conditions, phosphoramidates have zwitterionic character.[24,25] In buffered conditions near the pKa of the neighboring carboxylic acid, it is reasonable that this group transfers a proton to the phosphoramidate resulting in a more electrophilic phosphorus center susceptible to nucleophilic attack by water. However, in some cases (e.g., **6c**, **6d**, **8d**, **12b**, and **12c**), a transient species was observed in the ^{31}P NMR (at approximately -5.0 ppm) during the pH stability studies (see

Supporting Information, **Figure S1** as a representative example), which suggested that an intermediate mixed anhydride may be forming due to an intramolecular substitution at the phosphorus center (**Scheme 2B**) before being intercepted by water. Such putative cyclic mixed anhydrides have been proposed previously[26,27] but at this time, we have not determined if one of these two mechanisms predominates for the carboxylate-based scaffolds of this study in contrast to the pryidinium-based scaffolds previously reported.[18] Regardless of the mechanism (**Scheme 2A**,**B**), the data herein suggests that the stability of the phosphoramidates toward hydrolysis under mild pH conditions is correlated to the proximity of the neighboring carboxylic acid for efficient proton transfer or substitution through a transient cyclic species.

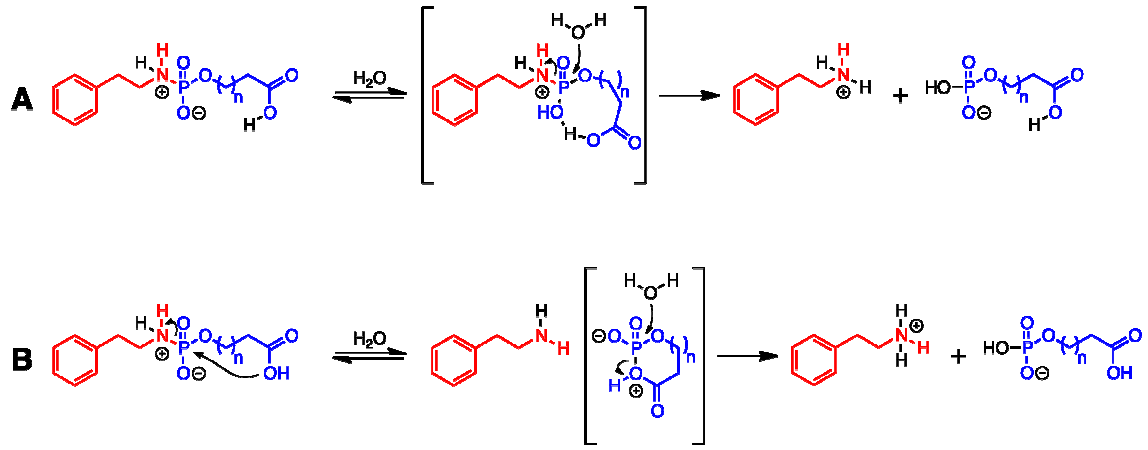

Scheme 2: Proposed intramolecular mechanisms of phosphoramidate hydrolysis.

A pronounced effect on stability was observed for the threonine-based compounds **7a**,**c**. Here we invoked the Thorpe-Ingold effect (commonly known as the gem-dimethyl effect), which is known to promote intramolecular interactions,[28-30] to destabilize the linker at mild pH conditions for more rapid drug release than the unsubstituted analogs **6a-d**. Indeed, the added methyl group promoted rapid hydrolysis of the model drug-linker conjugates **7a-d**. This is most notable for the aniline conjugate **7a** because the aniline conjugates exhibited little to no hydrolysis over 8 h. However, the added methyl group of the threonine residue in **7a**, in comparison to the serine analog **6a**, promoted rapid hydrolysis further demonstrating the tunability of the phosphoramidate-based drug-conjugate scaffold.

In addition to enhancing the rate of hydrolysis for the phosphoramidates through the Thorpe-Ingold effect, we also investigated the potential for a proximity effect by rigidifying the scaffold as in **12b**,**c**.[31] Indeed, substituting the homoserine residue of **8a-d** with the more rigid benzoate of **12b**,**c** resulted in model drug-conjugate scaffolds with a half-lives that were similar to the shorter serine-based homologs **7b**,**c**. These results, reminiscent of the *cis*-aconityl linker,[32] are encouraging and particularly attractive in that the pKa of the benzoate's carboxylate can be predictably tuned based on Hammett sigma constants.[33]

To further demonstrate that the proximal carboxylates were essential in promoting rapid hydrolysis of the phosphoramidate-based drug-conjugate scaffold, and to confirm that the scaffold could be protected from acidic hydrolysis in the form of a prodrug, we prepared **7c´** as the protected methyl ester of **7c**. Based on the pH-stability data for **7c´** compared to **7c**, it was confirmed that the carboxylate is key to promoting rapid hydrolysis of the phosphoramidate P-N bond. Moreover, the pH stability of **7c´** is interesting from a prodrug development perspective as it suggests that the phosphoramidate-based drug-conjugate scaffold can be protected as an ester prodrug for oral administration after which the scaffold can be activated by plasma or liver esterases.

Conclusions

In summary, we have again demonstrated that the phosphoramidate scaffold displays a wide range of stability at different pH values. Evaluation of our second-generation phosphoramidate-based drug-linker scaffolds further supports our hypothesis that a proximal carboxylic acid can promote hydrolysis of the P-N bond under mildly acidic conditions. Together with our pyridinium-based scaffolds,[18] the data suggests that any neighboring proton-donor may be employed to manipulate the lability of the P-N bond for controlled-release of an amine-containing drug, presumably through an intramolecular general-acid mechanism. In addition, we have found that the stability of the P-N bond can be further attenuated through the Thorpe-Ingold effect and rigidification. The benzoate-based scaffold **12** is particularly attractive in that the pKa of the neighboring carboxylic acid can be predictably modulated allowing for another degree of tunability. The stability profile of the ester analog **7c´** suggests that the scaffold could be used in prodrug applications and allow for oral administration.

Based on the data herein combined with our first-generation scaffolds,[18] it is expected

that cleavable linkers could be selected for particular properties for controlled-release applications such as amine type, stability under physiological conditions, or release rates at various pH values. For example, it is envisioned that **8d** could serve as a candidate linker scaffold for ADC applications with a secondary amine-containing drug (e.g., MMAE). Little to no detectable hydrolysis of **8d** at pH 7.4 was observed over 8 h whereas the $t_{1/2}$ was 6.22 h at pH 5.5. In the context of small-molecule drug conjugates (SMDCs), the more labile scaffolds, such as **6c** (pH 7.4 $t_{1/2}$ = 13.1 h; pH 5.5 $t_{1/2}$ = 0.76 h), would be better matched to the *in vivo* clearance profiles of small-molecules.

In conclusion, we expect the modular tunability of our phosphoramidate scaffold to find broad applicability in various controlled drug-release applications such as ADCs or SMDCs, drug-eluting stents, prodrugs, as well as intracellular trafficking studies in which pH changes can trigger the release of turn-on dyes. Having previously demonstrated that the pyridinium group[18] and now the benzoate group can function as a neighboring proton donor to promote phosphoramidates hydrolysis, it is envisioned that these scaffolds offer the advantage of subtle fine-tuning of amine-release kinetics through substitution effects on the aromatic rings.

Material and methods

pH Stability Studies. Samples were prepared using 5 mg of compound dissolved in 100 µL Milli-Q water, which was mixed with 400 µL of a 1 M buffer. Buffers were chosen based for specific pH values; 4-(2-hydroxyethyl)-1-piperazineethanesulfonic acid (HEPES, pH 7.4), succinic acid (pH 5.5), and citric acid (pH 3.0). Each buffer was prepared and equilibrated to ±0.01 pH with 1M NaOH or 1M HCl on an AB15 Accumet Basic pH Meter equipped with an accuTupH Ag/AgCl pH probe (Fisher Scientific, Sommerville, NJ).

Stability studies were performed using ^{31}P NMR on a Varian 400 MHz (Agilent Technologies, Santa Clara, CA). The instrument was equilibrated to 37^{o}C, with an acquisition of 64 scans, a relaxation delay of 1s, an observed pulse of 3.41 µs at 45^{o}, and a pre-acquisition delay of either 34 s or 184 s. The instrument was locked to an internal standard, triphenylphosphine oxide (TPPO, 40 mM in DMSO-d_6), in an axial capillary positioned within the sample solution. Stability data was collected for 8 h, or until complete decay was observed. After data acquisition was complete, all ^{31}P chemical shifts were referenced to the internal standard (TPPO, 27 ppm) and the phase adjusted accordingly.

NMR experiment files were loaded into the software MestReNova v10.0. Phase correction, baseline-fitting, and Savitzy-Golay smoothing were performed in the NMR software. Regions corresponding to the control, starting material, and the product peak were then exported into the software IGOR Pro 6.37 (Wavemetrics, Lake Oswego, OR, USA). The intensities of each spectra were normalized to the intensity of the control compound. A first order decaying exponential fitting function (**Equation 1**[34,35]), using the Levenberg-Marquardt algorithm, was applied to a plot of intensity versus time of the decaying parent compound. If the function returned a successful fit, the half-life $\left(t_{1/2}\right)$ of each compound was then calculated by multiplying the returned coefficient tau (τ) by ln 2.

$$y(x) = y_0 + A\, e^{-\left(\frac{x-x_0}{\tau}\right)} \qquad \textbf{Equation 1}$$

Synthesis. All solvents used in reactions were anhydrous and obtained from commercial sources or freshly distilled over calcium hydride. ^{1}H, ^{13}C, and ^{31}P NMR spectra were recorded on a Varian 300 MHz , 400 or 600 MHz spectrometer. ^{1}H NMR chemical shifts are relative to TMS (δ=0.00 ppm), $CDCl_3$ (δ=7.26 ppm), CD_3OD (δ=3.31 ppm) or D_2O (δ=4.79 ppm). ^{13}C NMR chemical shifts were relative to $CDCl_3$ (δ=77.23 ppm) or CD_3OD (δ=49.15 ppm). High Resolution Mass spectrometry (HRMS) spectra were obtained on an Applied Biosystems 4800 MALDI- TOF/TOF mass spectrometer (Applied Biosystems, Foster City, CA).

General procedure for synthesis of H-Phosphonates (20-25). **General procedure for synthesis of H-phosphonates 20-25.** The alcohol **14-20** (0.893 g, 2.85 mmol, 1 eq) was dissolved in freshly distilled pyridine (4 mL) under Ar (g) and cooled to -5 ^{o}C. A 50% v/v solution of diphenylphosphite (1.65 mL, 4.23 mmol, 1.5 eq) in freshly distilled pyridine under Ar (g) was added dropwise via syringe to the cooled alcohol solution. The mixture was allowed to warm to room temperature until the alcohol was consumed. Benzyl alcohol (0.740 mL, 7.12 mmol, 2.5 eq) was added via syringe, and the solution was stirred at room temperature for 4 h. The crude mixture was taken up with EtOAc (50 mL) and washed sequentially with 10% HCl (3X, 50 mL) to remove the pyridine and brine (50 mL). The organic layer was dried over anhydrous Na_2SO_4 (s) and the solvent was removed *in vacuo*. The product was obtained via silica flash chromatography with EtOAc:Hex as the eluent, dried overnight under *high vacuo*, then advanced immediately without further characterization (36.4-72.5% yield).

General Atherton-Todd method for phosphoramidates 26-31. All phosphoramidates are obtained as a mixture of enantiomers/diastereomers. Chirality on the phosphorus atom is lost after removal of benzyl esters. All ^{31}P and ^{13}C NMR are decoupled to ^{1}H. Amines used as the hydrochloride salt were prepared by adding the amine to a cooled solution of 4 N HCl in 1,4-dioxanes and subsequently filtered and washed with dry diethyl ether.

Method A: A solution of the H-phosphonate (0.390 mmol, 1.0 eq) in dry solvent (CH_3CN or CH_2Cl_2), 2.0 mL, was cooled to -15 ^oC under Ar (g). Carbon tetrachloride (CCl_4) or bromotrichloromethane ($BrCCl_3$), 2.0 mL, was added via syringe and the solution was stirred for 15 min at -15 ^oC. A cooled solution of the amine hydrochloride (0.40 mmol, 1.02 eq) and Et_3N (0.790 mmol, 2.0 eq) in dry solvent (CH_3CN or CH_2Cl_2) under Ar (g) was transferred dropwise via syringe to the H-phosphonate solution. The reaction was allowed to warm to room temperature and monitored the consumption of the H-phosphonate. The crude solution was concentrated *in vacuo*. The residue was diluted with EtOAc (50 mL) and washed sequentially with 10% HCl (50mL) and brine (50 mL). The organic layer was dried over anhydrous Na_2SO_4 (s) and the solvent was removed *in vacuo*. The pure phosphoramidate was isolated by silica or reversed-phase flash chromatography if required (25.2-99.1%).

Method B: A solution of the H-phosphonate (0.720 mmol, 1.0 eq) in dry CH_2Cl_2 (7.2 mL) was cooled to -15 ^oC under Ar (g). $BrCCl_3$ (7.2 mL) was added via syringe and the solution was stirred for 15 min at -15 ^oC. A cooled solution of the amine hydrochloride (0.800 mmol, 1.1 eq) and catalytic amount of 4-DMAP (0.072 mmol, 0.1 eq) in dry CH_2Cl_2 under Ar (g) was transferred dropwise via syringe to the H-phosphonate solution. Et_3N (1.520 mmol, 2.1 eq) was added dropwise, and the solution was immediately stirred at room temperature until consumption of the phosphite. The crude solution was diluted with CH_2Cl_2 (50 mL) and washed sequentially with 10% HCl (50 mL) and brine (50 mL). The organic layers were collected and dried over anhydrous Na_2SO_4 (s) and the solvent was removed *in vacuo*. The pure phosphoramidates were purified by either silica or reversed-phase chromatography (10.1-33.8%).

General procedure for global deprotection for linkers 6-11. To a solution of the phosphoramidate (0.09 mmol) in 1,4-dioxanes was added $KHCO_3$ (s) (0.18 mmol, 1.0 eq per benzyl group) in ddH_2O and 10% Pd/C (0.019 mmol). The mixture was stirred vigorously, purged with N_2 (g) and then charged with H_2 (g) under balloon pressure at room temperature for 1-2 h. The crude reaction mixture was filtered through a 0.2 μm PTFE micropore filtration disk

(Whatman) and the filter was then washed with ddH_2O. The solvent was lyophilized to yield the pure product as the potassium salt in quantitative yield.

Supporting Information

A table of half-lives for compounds **6-12,** characterization data for intermediates **14-31** and final compounds **6-12** are available in the Supporting Information.

Acknowledgements

This work was supported in part by the National Institutes of Health (R01 CA140617) and the Washington State University Commercialization Gap Fund (CGF). The authors extend their gratitude for technical assistance to G. Helms and W. Hiscox (WSU Center for NMR Spectroscopy) and Gerhard Munske (WSU lab Bioanalysis and Biotechnology for Mass Spectrometry).

References

(1) Albers, A. E., Garofalo, A. W., Drake, P. M., Kudirka, R., de Hart, G. W., Barfield, R. M., Baker, J., Banas, S., and Rabuka, D. (2014) Exploring the effects of linker composition on site-specifically modified antibody-drug conjugates. *European journal of medicinal chemistry*.

(2) Chari, R. V., Miller, M. L., and Widdison, W. C. (2014) Antibody-drug conjugates: an emerging concept in cancer therapy. *Angew Chem Int Ed Engl 53*, 3796-827.

(3) Nyman, E. S., and Hynninen, P. H. (2004) Research advances in the use of tetrapyrrolic photosensitizers for photodynamic therapy. *Journal of Photochemistry and Photobiology B: Biology 73*, 1-28.

(4) Panowksi, S., Bhakta, S., Raab, H., Polakis, P., and Junutula, J. R. (2014) Site-specific antibody drug conjugates for cancer therapy. *mAbs 6*, 34-45.

(5) Lyon, R. P., Setter, J. R., Bovee, T. D., Doronina, S. O., Hunter, J. H., Anderson, M. E., Balasubramanian, C. L., Duniho, S. M., Leiske, C. I., Li, F., and Senter, P. D. (2014) Self-hydrolyzing maleimides improve the stability and pharmacological properties of antibody-drug conjugates. *Nature biotechnology 32*, 1059-62.

(6) Pillow, T. H., Tien, J., Parsons-Reponte, K. L., Bhakta, S., Li, H., Staben, L. R., Li, G., Chuh, J., Fourie-O'Donohue, A., Darwish, M., Yip, V., Liu, L., Leipold, D. D., Su, D., Wu, E., Spencer, S. D., Shen, B. Q., Xu, K., Kozak, K. R., Raab, H., Vandlen, R., Lewis Phillips, G. D., Scheller, R. H., Polakis, P., Sliwkowski, M. X., Flygare, J. A., and Junutula, J. R. (2014) Site-Specific Trastuzumab Maytansinoid Antibody-Drug Conjugates with Improved Therapeutic Activity through Linker and Antibody Engineering. *Journal of medicinal chemistry 57*, 7890-9.

(7) Tumey, L. N., Charati, M., He, T., Sousa, E., Ma, D., Han, X., Clark, T., Casavant, J., Loganzo, F., Barletta, F., Lucas, J., and Graziani, E. I. (2014) Mild Method for

Succinimide Hydrolysis on ADCs: Impact on ADC Potency, Stability, Exposure, and Efficacy. *Bioconjugate chemistry 25*, 1871-80.

(8) Behrens, C. R., and Liu, B. (2014) Methods for site-specific drug conjugation to antibodies. *mAbs 6*, 46-53.

(9) Francisco, J. A., Cerveny, C. G., Meyer, D. L., Mixan, B. J., Klussman, K., Chace, D. F., Rejniak, S. X., Gordon, K. A., DeBlanc, R., Toki, B. E., Law, C. L., Doronina, S. O., Siegall, C. B., Senter, P. D., and Wahl, A. F. (2003) cAC10-vcMMAE, an anti-CD30-monomethyl auristatin E conjugate with potent and selective antitumor activity. *Blood 102*, 1458-65.

(10) Flygare, J. A., Pillow, T. H., and Aristoff, P. (2013) Antibody-drug conjugates for the treatment of cancer. *Chemical biology & drug design 81*, 113-21.

(11) Foehrenbacher, A., Patel, K., Abbattista, M. R., Guise, C. P., Secomb, T. W., Wilson, W. R., and Hicks, K. O. (2013) The Role of Bystander Effects in the Antitumor Activity of the Hypoxia-Activated Prodrug PR-104. *Front Oncol 3*, 263.

(12) Wu, W., Luo, Y., Sun, C., Liu, Y., Kuo, P., Varga, J., Xiang, R., Reisfeld, R., Janda, K. D., Edgington, T. S., and Liu, C. (2006) Targeting cell-impermeable prodrug activation to tumor microenvironment eradicates multiple drug-resistant neoplasms. *Cancer research 66*, 970-80.

(13) Dosio, F., Brusa, P., and Cattel, L. (2011) Immunotoxins and anticancer drug conjugate assemblies: the role of the linkage between components. *Toxins (Basel) 3*, 848-83.

(14) Tuma, R. S. (2011) Enthusiasm for antibody-drug conjugates. *Journal of the National Cancer Institute 103*, 1493-4.

(15) Sassoon, I., and Blanc, V. (2013) Antibody-drug conjugate (ADC) clinical pipeline: a review. *Methods in molecular biology 1045*, 1-27.

(16) Ducry, L., and Stump, B. (2010) Antibody-drug conjugates: linking cytotoxic payloads to monoclonal antibodies. *Bioconjugate chemistry 21*, 5-13.

(17) Nolting, B. (2013) Linker technologies for antibody-drug conjugates. *Methods in molecular biology 1045*, 71-100.

(18) Choy, C. J., Geruntho, J. J., Davis, A. L., and Berkman, C. E. (2016) Tunable pH-Sensitive Linker for Controlled Release. *Bioconjugate chemistry 27*, 824-830.

(19) Capon, B. (1975) Neighbouring Group Participation, in *Proton-Transfer Reactions* (Caldin, E., and Gold, V., Eds.) pp 339-384, Springer US, Boston, MA.

(20) Kirby, A. J., Lima, M. F., da Silva, D., Roussev, C. D., and Nome, F. (2006) Efficient Intramolecular General Acid Catalysis of Nucleophilic Attack on a Phosphodiester. *Journal of the American Chemical Society 128*, 16944-16952.

(21) Fersht, A. R., and Kirby, A. J. (1967) Intramolecular general acid catalysis of ester hydrolysis by the carboxylic acid group. *Journal of the American Chemical Society 89*, 5961-5962.

(22) Orth, E. S., Brandão, T. A. S., Souza, B. S., Pliego, J. R., Vaz, B. G., Eberlin, M. N., Kirby, A. J., and Nome, F. (2010) Intramolecular Catalysis of Phosphodiester Hydrolysis by Two Imidazoles. *Journal of the American Chemical Society 132*, 8513-8523.

(23) Bender, M. L., and Lawlor, J. M. (1963) Isotopic and Kinetic Studies of the Mechanism of Hydrolysis of Salicyl Phosphate. Intramolecular General Acid Catalysis. *Journal of the American Chemical Society 85*, 3010-3017.

(24) Benkovic, S. J., and Schray, K. J. (1978) The Mechanism of Phosphoryl Transfer, in *Transition States of Biochemical Processes* (Gandour, R. D., and Schowen, R. L., Eds.) pp 493-527, Springer US, Boston, MA.

(25) Zakirova, N. F., Shipitsyn, A. V., Jasko, M. V., Prokofjeva, M. M., Andronova, V. L., Galegov, G. A., Prassolov, V. S., and Kochetkov, S. N. (2012) Phosphoramidate derivatives of acyclovir: synthesis and antiviral activity in HIV-1 and HSV-1 models in vitro. *Bioorganic & medicinal chemistry 20*, 5802-9.

(26) Jacobsen, N. E., and Bartlett, P. A. (1983) Cyclic phosphonic-carboxylic imides and anhydrides as reactive intermediates. 2. Solvolysis of N-(hydroxy(methyl)phosphinothioyl)-L-phenylalanine derivatives. *Journal of the American Chemical Society 105*, 1619-1626.

(27) Mallari, J. P., Choy, C. J., Hu, Y., Martinez, A. R., Hosaka, M., Toriyabe, Y., Maung, J., Blecha, J. E., Pavkovic, S. F., and Berkman, C. E. (2004) Stereoselective inhibition of glutamate carboxypeptidase by organophosphorus derivatives of glutamic acid. *Bioorganic & medicinal chemistry 12*, 6011-20.

(28) Jung, M. E., and Piizzi, G. (2005) gem-disubstituent effect: theoretical basis and synthetic applications. *Chemical reviews 105*, 1735-66.

(29) DeWit, M. A., and Gillies, E. R. (2011) Design, synthesis, and cyclization of 4-aminobutyric acid derivatives: potential candidates as self-immolative spacers. *Organic & biomolecular chemistry 9*, 1846-54.

(30) McGuigan, C., Tsang, H.-W., Cahard, D., Turner, K., Velazquez, S., Salgado, A., Bidois, L., Naesens, L., De Clercq, E., and Balzarini, J. (1997) Phosphoramidate derivatives of d4T as inhibitors of HIV: The effect of amino acid variation. *Antiviral Research 35*, 195-204.

(31) Liang, G. B., Desper, J. M., and Gellman, S. H. (1993) Effects of backbone rigidification on intramolecular hydrogen bonding in a family of diamides. *Journal of the American Chemical Society 115*, 925-938.

(32) Shen, W.-C., and Ryser, H. J. P. (1981) Cis-aconityl spacer between daunomycin and macromolecular carriers: A model of pH-sensitive linkage releasing drug from a lysosomotropic conjugate. *Biochemical and Biophysical Research Communications 102*, 1048-1054.

(33) Hansch, C., Leo, A., and Taft, R. W. (1991) A survey of Hammett substituent constants and resonance and field parameters. *Chemical reviews 91*, 165-195.

(34) Kalogiannis, M., Hsu, E., Willie, J. T., Chemelli, R. M., Kisanuki, Y. Y., Yanagisawa, M., and Leonard, C. S. (2011) Cholinergic Modulation of Narcoleptic Attacks in Double Orexin Receptor Knockout Mice. *PLoS ONE 6*, e18697.

(35) Hoerter, J. A., and Walter, N. G. (2007) Chemical modification resolves the asymmetry of siRNA strand degradation in human blood serum. *RNA 13*, 1887-93.

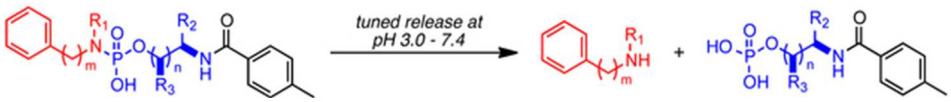

6a-d: m=0 or 2; n=1; R_1=H or Me; R_2=CO_2H; R_3=H
7a-c: m=0 or 2; n=1; R_1=H or Me; R_2=CO_2H; R_3=Me
7c': m=2, ; R_1=H; R_2=CO_2Me
8a-d: m=0 or 2; n=2; R_1=H or Me; R_2=CO_2H; R_3=H
9c-d: m=2; n=3; R_1=H or Me; R_2=CO_2H; R_3=H
10a-d: m=0 or 2; n=1; R_1=H or Me; R_2=R_3=H
11a-d: m=0 or 2; n=2; R_1=H or Me; R_2=R_3=H

Graphical Abstract
56x16mm (300 x 300 DPI)

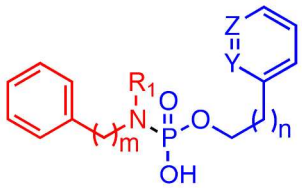

1: n=1; Y=Z=C; m=2; R_1=Me
1': n=2; Y=Z=C; m=2; R_1=Me
2 a-d: n=1; Y=N; Z=C
3 a-d: n=1; Y=C; Z=N
4 a-d: n=2; Y=N; Z=C
5 a-d: n=2; Y=C; Z=N

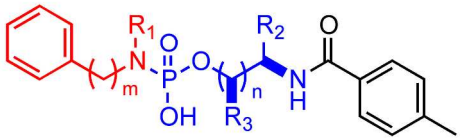

6a-d: m=0 or 2; n=1; R_1=H or Me; R_2=CO_2H; R_3=H
7a-c: m=0 or 2; n=1; R_1=H or Me; R_2=CO_2H; R_3=Me
7c': m=2, ; R_1=H; R_2=CO_2Me
8a-d: m=0 or 2; n=2; R_1=H or Me; R_2=CO_2H; R_3=H
9c-d: m=2; n=3; R_1=H or Me; R_2=CO_2H; R_3=H
10a-d: m=0 or 2; n=1; R_1=H or Me; R_2=R_3=H
11a-d: m=0 or 2; n=2; R_1=H or Me; R_2=R_3=H

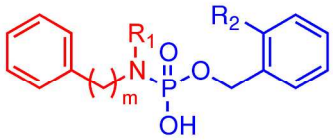

12b: m=0; R_1=Me; R_2=CO_2H
12c: m=2; R_1=H; R_2=CO_2H

Phosphoramidate-based pH-programmable cleavable linkers
Figure 1
165x326mm (300 x 300 DPI)

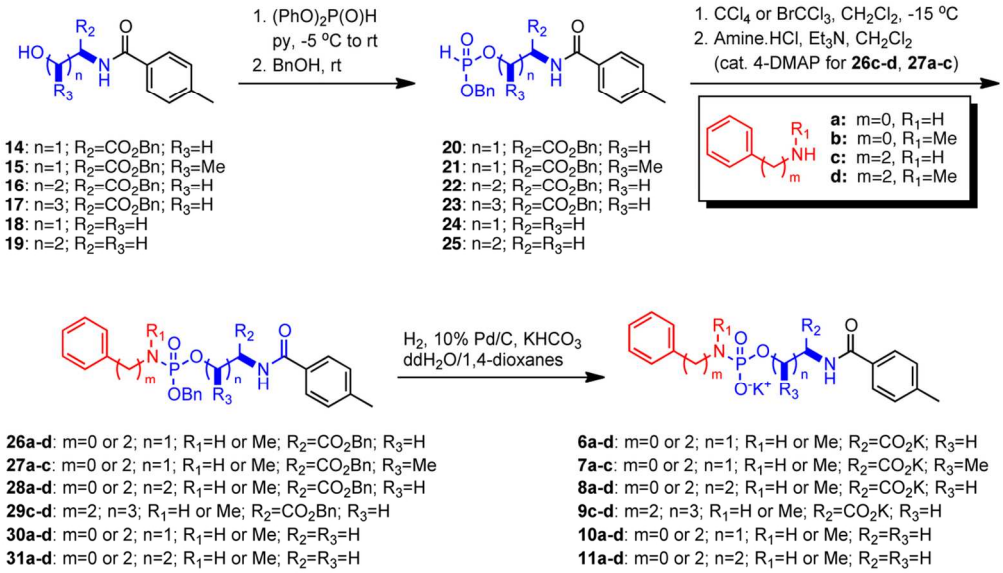

14: n=1; R_2=CO_2Bn; R_3=H
15: n=1; R_2=CO_2Bn; R_3=Me
16: n=2; R_2=CO_2Bn; R_3=H
17: n=3; R_2=CO_2Bn; R_3=H
18: n=1; R_2=R_3=H
19: n=2; R_2=R_3=H

20: n=1; R_2=CO_2Bn; R_3=H
21: n=1; R_2=CO_2Bn; R_3=Me
22: n=2; R_2=CO_2Bn; R_3=H
23: n=3; R_2=CO_2Bn; R_3=H
24: n=1; R_2=R_3=H
25: n=2; R_2=R_3=H

26a-d: m=0 or 2; n=1; R_1=H or Me; R_2=CO_2Bn; R_3=H
27a-c: m=0 or 2; n=1; R_1=H or Me; R_2=CO_2Bn; R_3=Me
28a-d: m=0 or 2; n=2; R_1=H or Me; R_2=CO_2Bn; R_3=H
29c-d: m=2; n=3; R_1=H or Me; R_2=CO_2Bn; R_3=H
30a-d: m=0 or 2; n=1; R_1=H or Me; R_2=R_3=H
31a-d: m=0 or 2; n=2; R_1=H or Me; R_2=R_3=H

6a-d: m=0 or 2; n=1; R_1=H or Me; R_2=CO_2K; R_3=H
7a-c: m=0 or 2; n=1; R_1=H or Me; R_2=CO_2K; R_3=Me
8a-d: m=0 or 2; n=2; R_1=H or Me; R_2=CO_2K; R_3=H
9c-d: m=2; n=3; R_1=H or Me; R_2=CO_2K; R_3=H
10a-d: m=0 or 2; n=1; R_1=H or Me; R_2=R_3=H
11a-d: m=0 or 2; n=2; R_1=H or Me; R_2=R_3=H

Synthesis of model drug-linker phosphoramidates
Scheme 1
115x66mm (300 x 300 DPI)

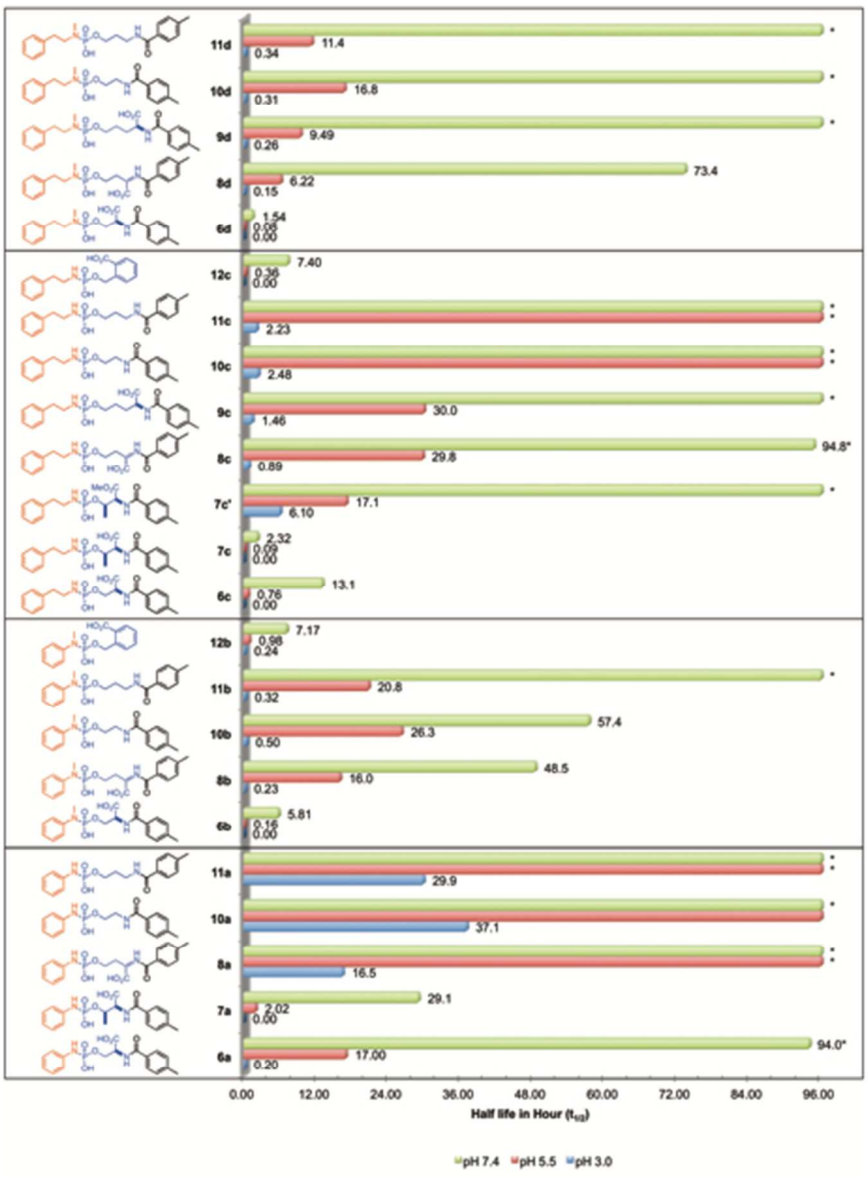

Stability of model drug-linker phosphoramidates at pH 3.0, 5.5, and 7.4 (37 oC). *No detectable hydrolysis observed over 8 hrs.

Figure 3

162x225mm (72 x 72 DPI)

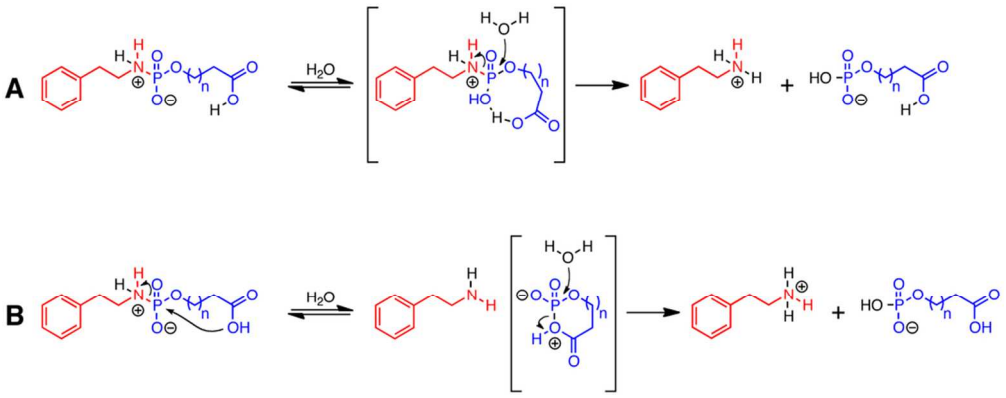

Proposed intramolecular mechanisms of phosphoramidate hydrolysis.
Scheme 2
90x35mm (300 x 300 DPI)